
Dynamics of Air Pollution and its Dispersion in a Topographically Constrained Urban Area: A Case Study of Kathmandu Valley

Rajib Pokhrel^{1*}

¹ School of Engineering, Faculty of Science and Technology, Pokhara University, Nepal

*Corresponding email: rajibp@pu.edu.np



Pokhara Engineering College Journal (ISSN: 3021-9795, print) and (ISSN: 3059-9628, online), Copyright © [2026] The Author(s). Published by Pokhara Engineering College, distributed under the terms of the Creative Commons Attribution 4.0 International License (CC BY-NC 4.0).

Received: 10- February-2026; Revised: 28- February-2026; Accepted: 20- March-2026

DOI: <https://doi.org/10.3126/pecj.v3i1.93523>

Abstract

Kathmandu, one of the world's prominent cultural and touristic cities, has undergone rapid urbanization over recent decades, creating substantial challenges for environmental quality management amid accelerating population growth and infrastructure development. This study examines the meteorological characteristics, ambient air quality, and pollutant dispersion mechanisms in the Kathmandu Valley through an integrated analysis of primary observations, secondary datasets, and numerical simulations. Meteorological and air quality data from multiple monitoring stations indicate strong seasonal variability, with daily mean temperatures ranging from approximately 10 °C to 24 °C. Higher wind speeds (~6 m/s) prevail in spring and summer, while calm winds dominate autumn and winter, accounting for more than 50% of observations. Particulate matter concentrations frequently exceed guideline levels, with PM₁₀ surpassing 100 µg/m³ and PM_{2.5} reaching up to 80 µg/m³, particularly during winter, when pollution levels are more than twice those observed in spring and autumn. Monsoonal rainfall significantly suppresses particulate concentrations during summer. Source characterization highlights the predominance of soil-based dust, which accounts for over 60% of non-ionic components and approximately 25% of PM₁₀, alongside a relatively high black carbon fraction (~17%). Numerical simulations reveal a pronounced diurnal mountain–valley breeze system, with mountain breezes dominating at night and valley breezes prevailing during the day. Stronger north–south airflow governs pollutant transport, causing emissions from the northern and central Valley to disperse widely, while pollutants originating from southern and southeastern sources exhibit limited penetration into the urban core.

Keywords: *Meteorology; Mountain/Valley Breeze; Air Pollution; Dispersion Model, UHI*

1. Introduction

Kathmandu Valley comprises three administrative districts and covers an area of 933.73 km², accommodating approximately 3 million inhabitants according to the Central Bureau of Statistics (CBS, 2021). Over the past three decades, the Valley has experienced rapid population growth, extensive spatial expansion, and intense urban densification. Collectively,

the three districts of Kathmandu Valley exhibit an average population density of approximately 97 persons per km²; however, Kathmandu Metropolitan City alone records an exceptionally high density of about 13,225 persons per km². The annual population growth rate in the Valley exceeded 4.5%, significantly surpassing the national average growth rate of approximately 2.5% during the same period (Central Bureau of Statistics, Nepal, 2001). This accelerated urbanization has posed substantial challenges to environmental management, particularly in maintaining air quality and overall environmental health. According to reports by the World Health Organization (WHO), Kathmandu Valley is among the most polluted urban areas in Asia, with persistently high levels of air pollution arising from road dust, vehicular emissions, brick kilns, and other airborne particulate sources throughout the year.



Figure 1: The geographic location of the Kathmandu Valley in Nepal.

The air quality of the Valley was improved in 2003, and it was aggravated again in 2005. There was a slight improvement in air quality in 2006, but it has been steadily worsening since 2007 (Chaudhari, 2010). Dust particles, oxides of nitrogen (NO_x), carbon monoxide (CO), sulfur oxides (SO_x), Hydrocarbons (HCs), benzenes, etc., are the major pollutants in the valley air (Panday et al., 2009). The increased exposure to PM₁₀ is associated with various adverse health effects, such as respiratory diseases, cardiovascular mortality, morbidity, and probably malignant lung diseases (Goldberg et al., 2006; Chang et al., 2005; Kan et al., 2003; Donaldson et al., 2001). Fine particulate matter is mostly generated from vehicle emissions, and the secondary pollution aggravates the atmospheric visibility by scattering or absorbing the visible light (Pokhrel et al., 2011, and Pokhrel et al., 2021). Similarly, the gaseous pollutants in the air cause severe physical environmental and health effects (Panday et al., 2009). In addition, the inversion height is below the surrounding mountains, and it plays a role like a lid for the Valley

air, mostly in the winter season when the air pollution is accumulated in the confined boundary, and the air quality is aggravated further (Pudasainee et al., 2010; Sapkota, 2002; Sharma, 1997).

A large number of vehicles, brick kiln factories, concrete gridding factories, etc., are the major sources of air pollution in the Kathmandu valley. The brick kiln industry is one of the major air pollution sources, where brick is one of the major construction materials in the valley and its neighboring areas (Pokhrel and Lee, 2014). The total production of 350 million bricks was the major single source of sulfur dioxide and suspended particulate matter in the valley. It contributes over 60% of emissions and is responsible for the 31% of TSP (Total Suspended Particle) and 28 % of PM10 (Tuladhar et al., 2002; World Bank, 1997; Shrestha et al., 1996). Although it has a significant contribution to the valley air pollution, there is a lack of emission inventory data from each stage of brick production. Moreover, large numbers of construction works have been running around the valley area, which has also become one of the major emission sources.



(a) Satdobato – 30 Nov. 2016 (b) Road side dust at Chakrapath (C) Stack Emission

Figure 2: Air pollution situation and major sources in the Valley

2. Air Dispersion Model

Modeling technique is an essential tool for atmospheric environmental studies together with observational data. Models are divided into two types: physical and mathematical. The physical model is a small-scale, laboratory representation of the phenomena, and the mathematical model is the set of analytical/numerical algorithms addressing the physical and numerical aspects of the problems. Based on the quantitative and qualitative studies, the mathematical models are categorized into deterministic and statistical models. The deterministic models are based on fundamental mathematical descriptions of atmospheric processes, whereas the statistical models are based on semi-empirical statistical relations among available data and measurements.

For calculating the specific value of output based on certain input data, deterministic models are used. The statistical models are generally used to forecast or estimate the values by using statistical functions and the measurement values. In the case of atmospheric environmental studies, a large number of meteorological models and air pollution diffusion/dispersion models have been developed using different mathematical models. Various analytical models have been introduced to calculate the exact analytical solutions using mathematical formulas and observational data. In addition, the mathematical models can be numerical models, where the approximate numerical solutions are attained using numerical integration techniques. With the introduction of computer applications for scientific studies, numerical simulations based on mathematical models have been widely introduced since the 1970s. Later, the simulations are updated and the results are validated with observational data. Then the numerical simulation methods have been one of the most popular techniques for environmental forecasting, air pollution estimation, environmental impact assessment studies, etc. since few decades.

2.1. Gaussian approach

In 1991, the American Meteorological Society (AMS) and the U.S. Environmental Protection Agency (EPA) initiated a formal collaboration with the designed goal of introducing current planetary boundary layer (PBL) concepts into regulatory dispersion models. A working group (AMS/EPA Regulatory Model Improvement Committee, AERMIC) comprised of AMS and EPA scientists was organized for the collaborative effort. In most air quality applications, one is concerned with dispersion in the PBL, the turbulent air layer close to the earth's surface is controlled by the surface heating and friction and the overlying stratification. The PBL typically ranges from a few hundred meters in depth during nighttime to 1 – 2 km during daytime. Major developments in understanding the PBL began in the 1970's through numerical modeling, field observations, and laboratory simulations (Wyngaard, 1988). For the convective boundary layer (CBL), a milestone was Deardorff's (1972) numerical simulations, which revealed the CBL's vertical structure and important turbulence scales. Major insights into dispersion followed from laboratory experiments, numerical simulations, and field observations are described in Briggs (1988), Lamb (1982), and Weil (1988a).

In February 1991, the U.S. EPA, in conjunction with the AMS, held a workshop for state and EPA regional meteorologists on the parameterization of PBL turbulence and the state-of-the-art dispersion modeling. One of the outcomes of the workshop was the formation of AERMIC, and the major purpose of the AERMIC activity was to build upon the earlier model developments and to provide a state-of-the-art dispersion model for regulatory applications.

The early efforts of the AERMIC group were described by Weil (1992). The new model developed by AERMIC was aimed at short-range dispersion from stationary industrial sources, the same scenario handled by the EPA Industrial Source Complex Model, ISC3 (U.S. Environmental Protection Agency 1995). In addition, AERMIC selected the EPA's ISC3 Model for a major overhaul and the AERMIC's objective was to develop a complete replacement for ISC3 by (1) adopting ISC3's input/output computer architecture; (2) updating, where practical, antiquated ISC3 model algorithms with newly developed or current state-of-the-art modeling techniques; and (3) insuring that the source and atmospheric processes presently modeled by ISC3 will continue to be handled by the AERMIC Model (AERMOD) (EPA, 2002).

AERMOD currently contains new or improved algorithms for (1) dispersion in both the convective and stable boundary layers; (2) plume rise and buoyancy ; (3) plume penetration into elevated inversions; (4) computation of vertical profiles of wind, turbulence, and temperature; (5) the urban nighttime boundary layer; (6) the treatment of receptors on all types of terrain from the surface up to and above the plume height; (7) the treatment of building wake effects; (8) an improved approach for characterizing the fundamental boundary layer parameters; and (9) the treatment of plume meander (EPA, 2002).

AERMOD is a steady-state plume model. In a stable boundary layer (SBL), it assumes the concentration distribution to be Gaussian in both the vertical and horizontal. In the convective boundary layer (CBL), the horizontal distribution is also assumed to be Gaussian, but the vertical distribution is described with a bi-Gaussian probability density function (pdf). This behavior of the concentration distribution in the CBL was demonstrated by Willis and Deardorff (1981) and Briggs (1993). Additionally, in the CBL, AERMOD treats "plume lofting", whereby a portion of plume mass, released from a buoyancy source, rises to and remains near the top of the boundary layer before becoming mixed into the CBL.

2.2. Lagrangian approach

A2C (Atmospheric to Computational fluid dynamics) flow and A2C t&d (transport & diffusion) are the updated versions of HOTMAC and RAPTAD, respectively. The basic equations of HOTMAC for mean wind, temperature, mixing ratio of water vapor, and turbulence are similar to those used by Yamada (1981, 1985). It has the addition of nested grid capability and the effect of shadows produced by terrain. The terrain vertical coordinate system is used in this model in order to increase the accuracy in the treatment of surface boundary conditions.

$$z^* = \overline{H} \frac{z - z_g}{H - z_g} \quad (1)$$

Where z^* and z are the transformed and Cartesian vertical coordinates, respectively; z_g is ground elevation; the material surface top of the model in the z^* coordinate; and H , the corresponding height in the z - coordinate. The governing equations following the coordinate transformation are explained in Yamada 1978, 1981, Yamada et al., 1988, Yamada, 1999 and 2003. Puff concentration distributions are assumed in different forms, and one of the simplest ways is to assume a Gaussian distribution where variances are determined as the time integration of the velocity variances encountered over the history of the puff. The concentration level at a given time and place is calculated as the sum of the concentrations from each puff (Yamada, 1999). Concentration C at (X, Y, Z) is computed by using equation (2).

$$C(X, Y, Z) = \frac{Q\Delta t}{(2\pi)^{3/2}} \sum_{k=1}^N \frac{1}{\sigma_{xk} \sigma_{yk} \sigma_{zk}} \exp\left[-\frac{1}{2} \frac{(x_k - X)^2}{\sigma_{xk}^2}\right] \times \exp\left[-\frac{1}{2} \frac{(y_k - Y)^2}{\sigma_{yk}^2}\right] \\ \times \left\{ \exp\left[-\frac{1}{2} \frac{(y_k - Y)^2}{\sigma_{yk}^2}\right] + \exp\left[-\frac{1}{2} \frac{(z_k + Z - 2z_g)^2}{\sigma_{zk}^2}\right] \right\} \quad (2)$$

Where (x_k, y_k, z_k) is the location of the k^{th} puff, σ_{xk} , σ_{yk} and σ_{zk} are the standard deviations of a Gaussian distribution, and z_g is the ground elevation. A brief description of the RAPTAD model was reported in detail by Yamada et al. (1988) and Yamada (1998, 1999). The concept has already been introduced for analyzing the air flow dynamics in Pokhara Valley (Pokhrel, 2025), which shows that this algorithm can be useful for further study in the Kathmandu Valley too.

3. Methodology

3.1. Study site

Kathmandu, located between 27°37'30" N and 27°45'0" N Latitude and 85°15'0" E and 85°22'30" E Longitude, is about 1500 m above sea level and covers about 340 km². The cross-section of the Kathmandu valley is about 20 km north-to-south and 30 km east-to-west. Kathmandu valley has a bowl-like shape surrounded by four major mountains, namely Shivapuri, Phulchowki, Nagarjun, and Chandragiri at an elevation of approximately 1400 m from its base.

Four distinct seasons, viz. spring, summer, autumn, and winter, are observed in the Kathmandu valley. During the course of study, the temperature of the valley varied from 5°C to 32°C, and

dry air with low temperature was frequently observed during the winter season, whereas high humidity (more than 90%) and hot weather were observed in the summer season.

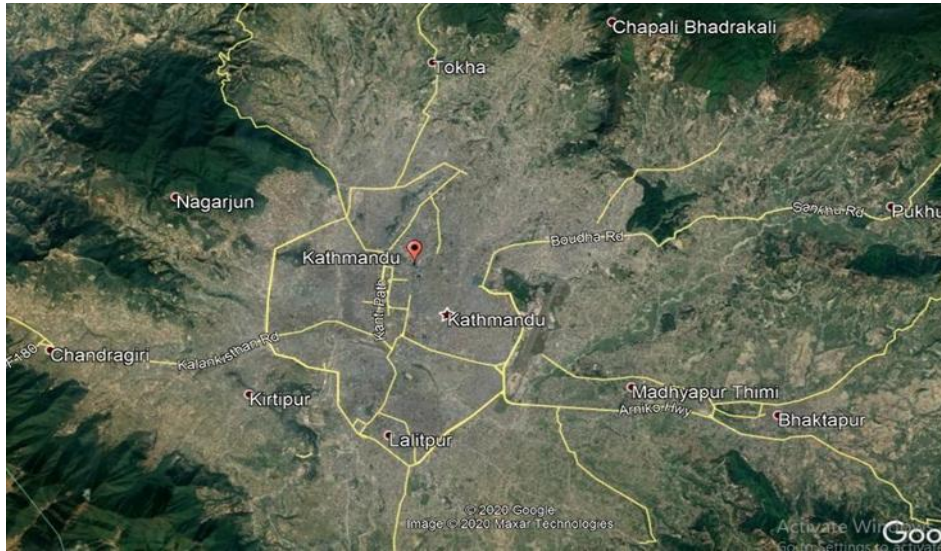


Figure 3: Study domain covering the central, residential/agricultural area and the surrounding high hills.

3.2. Research framework

The local climate of the Kathmandu valley is typical, as it is surrounded by the high hills. Most of the urban land is covered with built-up area and fine sandy soil, which can easily be blown by the wind, covering the top of the land surface. Air pollution, especially particulate matter (PM) dispersion pattern from the point/area source in the valley, has been studied. Meteorological data were collected from the Department of Hydrology and Meteorology. Surface topography and landuse data of 30” resolution were retrieved from USGS data. Major data and tools used in this study are summarized in the Figure 4.

Research Method	
<p><u>Data Preparation & Validation</u></p> <ul style="list-style-type: none"> ▪ Geographic data ▪ Land use data ▪ Surface meteorology data ▪ Validation of A2C Model <p><u>Methods</u></p> <ul style="list-style-type: none"> ▪ WMO and other secondary data ▪ USGS 30” resolution data 	<p><u>Numerical Study / Simulations</u></p> <ul style="list-style-type: none"> ▪ Modeling for pure breeze flow ▪ Factor affecting breeze flow <ul style="list-style-type: none"> - Surface topography ▪ Particle Dispersion Modeling <p><u>Major software</u></p> <ul style="list-style-type: none"> ▪ A2C flow / A2C t&d

Figure 5: Summary of the research methods.

3.3. Data collection

Meteorological data were obtained from established monitoring stations located at Tribhuvan International Airport (TIA) and Babarmahal, Kathmandu. As the TIA station records wind speed only and lacks wind direction measurements, wind data from the Babarmahal station were utilized to characterize airflow patterns through the construction of wind rose diagrams. Ambient air quality data, specifically PM₁₀ and PM_{2.5} concentrations, were collected from a network of existing monitoring stations, including Ratnapark, Phora Durbar (U.S. Embassy), Pulchowk, Bhaisipati, U.S. Embassy (Kathmandu), Shankapark, and Birendra School (Bhaktapur). Hourly averaged data spanning an entire year were compiled to examine both monthly and seasonal variations in air quality across the Kathmandu Valley. In addition, supplementary information from published secondary sources was consulted to define model boundary conditions and to support the interpretation of meteorological and air quality characteristics of the Valley. High-resolution topographic and land-use datasets (USGS 30") were employed as input for numerical modeling. Airflow dynamics and pollutant dispersion were simulated using a Lagrangian modeling framework (A2C Flow/t&d).

3.4 Air flow dynamics and dispersion modeling

Kathmandu Valley, characterized by its enclosed, basin-like topography, experiences persistently elevated levels of air pollution, with particularly high concentrations of particulate matter (PM) in the ambient atmosphere throughout the year. A comprehensive understanding of pollutant types, emission sources, and dispersion processes constitutes a fundamental prerequisite for the development of effective air quality management strategies. Previous studies have identified mobile sources, notably vehicular emissions; point sources, including brick kilns, cement and grinding industries, and commercial establishments; and area sources, such as forest fires and agricultural activities in surrounding regions, as the dominant contributors to air pollution in the Valley. Local meteorological conditions, especially airflow dynamics governed by valley - mountain circulation, play a critical role in the transport, accumulation, and dispersion of atmospheric pollutants within the study area. To simulate local airflow patterns and pollutant (puff) dispersion within the modeling domain, this study employs the Atmospheric to Computational Fluid Dynamics (A2C) Flow model coupled with the A2C Transport and Diffusion (A2C t&d) framework. Pollutants are treated as non-reactive primary species, and atmospheric chemical transformation processes occurring during transport and diffusion are not considered in this mesoscale simulation.

The modeling domain ($84^{\circ}35''$ E, $27^{\circ}03''$ N to $86^{\circ}10''$ E, $28^{\circ}12''$ N) was set using the USGS 30'' resolution topographic and land use data. It covers Kathmandu valley and its nearby mountains, as in Figure 5. The outer domain covers $150 \text{ km} \times 129 \text{ km}$ with a grid resolution of 3 km, the interim domain covers $75 \text{ km} \times 75 \text{ km}$ with a grid resolution of 1.5 km, and the innermost domain $33 \text{ km} \times 33 \text{ km}$ with a grid resolution of 500 m.

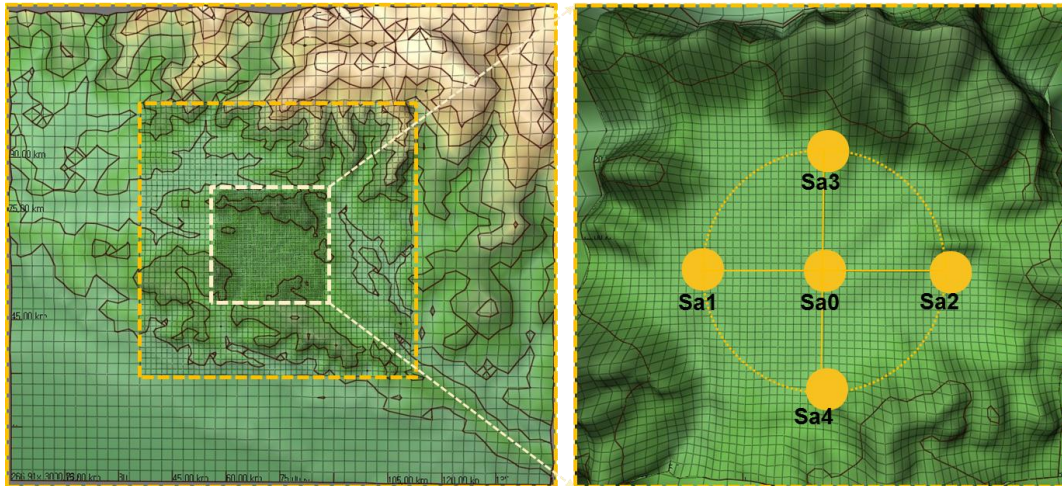


Figure 5: Modeling the domain in the inner grid shows the core Kathmandu Valley and its surroundings, respectively.

Modeling cases were designed by considering the local meteorological conditions, avoiding the external driving effect, such as the monsoon. 60-70 % of annual rainfalls occur during the monsoon season when external wind (monsoon wind) dominates the local wind. Modeling cases are designed at (a) Spring season – Pre-monsoon period, and (b) With the modification of landuse change for analyzing the UHI effects. Corresponding meteorological information has been used for setting the initial and boundary conditions.

3.4.1. Air flow dynamics and dispersion modeling – case study of spring season

The modeling period selected included mid-spring, i.e., April (Julian day 105 - 111), before the monsoon season when the effect of external wind is minimum in the study region. The potential temperature (298 K) and reference pressure (1013 mb) were referred based on the meteorology data monitored at the airport, and the inversion height (700 m) was referred from the literature (Regmi et al., 2003). The initial wind speed (0 m/s) was set by considering the pure breeze and the rest of the parameters were set as default suggested in the manual (HOTMAC® and RAPTAD® 7.8; Yamada Science & Art Corporation). In addition, the puff sources (Sa0, Sa1,

Sa2, Sa3 and Sa4) were set at the center, east, west, north and south part of the internal modeling domain (in the Kathmandu Valley) where Sa0 is located in-between Ratnapark and Dillibazaar (27.709N, 85.326E), Sa1 is located in Tahachal near to Chakrapath (27.702N, 85.282E), Sa2 is located at Bhaktapur area (27.6643N, 85.4460E), Sa3 is located at north part of the Valley (27.7469N, 85.335E) near to Narayan Gopal Chowk and Sa4 is located near to Sunakothe Lalitpur (27.632N, 85.3227E) as in the Figure 5. Elevation of all the puff sources was set 10 m above the surface, and the puff emission option was set continuous with the emission rate of 1 g/s. Moreover, the nudging option was set active to minimize the effect of initial and boundary conditions, and the earth rotation was set active by considering the solar angle and the gravity effect on air flow.

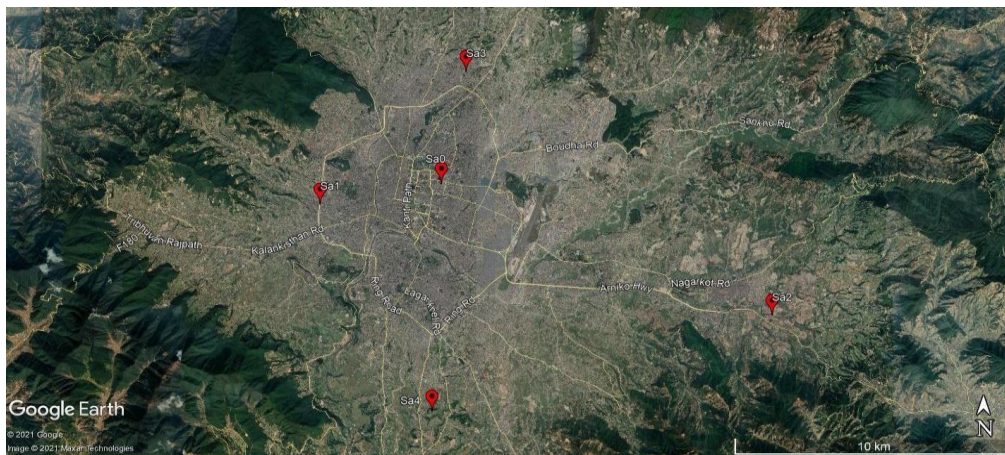


Figure 6: Geographic position of puff sources in Google Map.

3.4.2. Impact of landuse change on local breeze flow

With the urbanization, the landuse pattern of the Kathmandu Valley has been changing rapidly. The fertile irrigated cropped land has been changed to a built-up area where the surface characteristics, such as roughness coefficient, albedo, soil moisture, surface specific heat capacity, anthropogenic heat, etc., may be changed. The variation of surface characteristics may change the air flow and air dispersion characteristics of the valley; therefore three cases were simulated in the study by considering irrigated crop landuse, mixed landuse and urban landuse. The surface characteristics were set based on the value suggested from the manual, based on USGS data, and the innermost domain covering the valley basin only. Further simulation was carried out by setting the boundary condition to the same as in the case study of the spring season.

Table 1: Parameters affecting the local air flow.

S.N.	Landuse Type	Anthropogenic Heat (W/m ²)	Specific Heat (J/kgK)	Surface Albedo
1	USGS landuse (mixed)	0 -50	800 – 4186	0.03 – 0.3
2	Irrigated farm land	0	3650	0.2
3	Urban land	50	879	0.15

Source: USGS landuse data for Kathmandu Valley. The index values vary with the change of landuse type.

Numerous studies were carried out to study the Urban Heat Island (UHI) in different parts of the world, where waste heat from the facilities plays an important role in the formation of UHI. The amount of additional anthropogenic heat in the landside proportionally increases with the rate of urbanization. There might exist a difference in thermal properties, especially in the landside before and after the period of urbanization. Moreover, thermodynamic properties (heating and cooling properties) are dependent on the specific heat capacity of the material. The landuse and land surface material vary with the level of urbanization and the trend of adopting the construction material. Therefore, the specific heat capacity and the surface moisture of the land surface are also modified as per the data mentioned in the table. The albedo of typical materials for the visible light range from 0.9 for fresh snow to 0.04 for charcoal. The albedo for an ideal black body reaches to zero. The albedo for most of the land area ranges from 0.1 to 0.4. According to the USGS landuse data, the albedo for irrigated farming land and urban land are 0.2 and 0.15, respectively.

4. Results and Discussion

4.1. Meteorology of the Kathmandu Valley

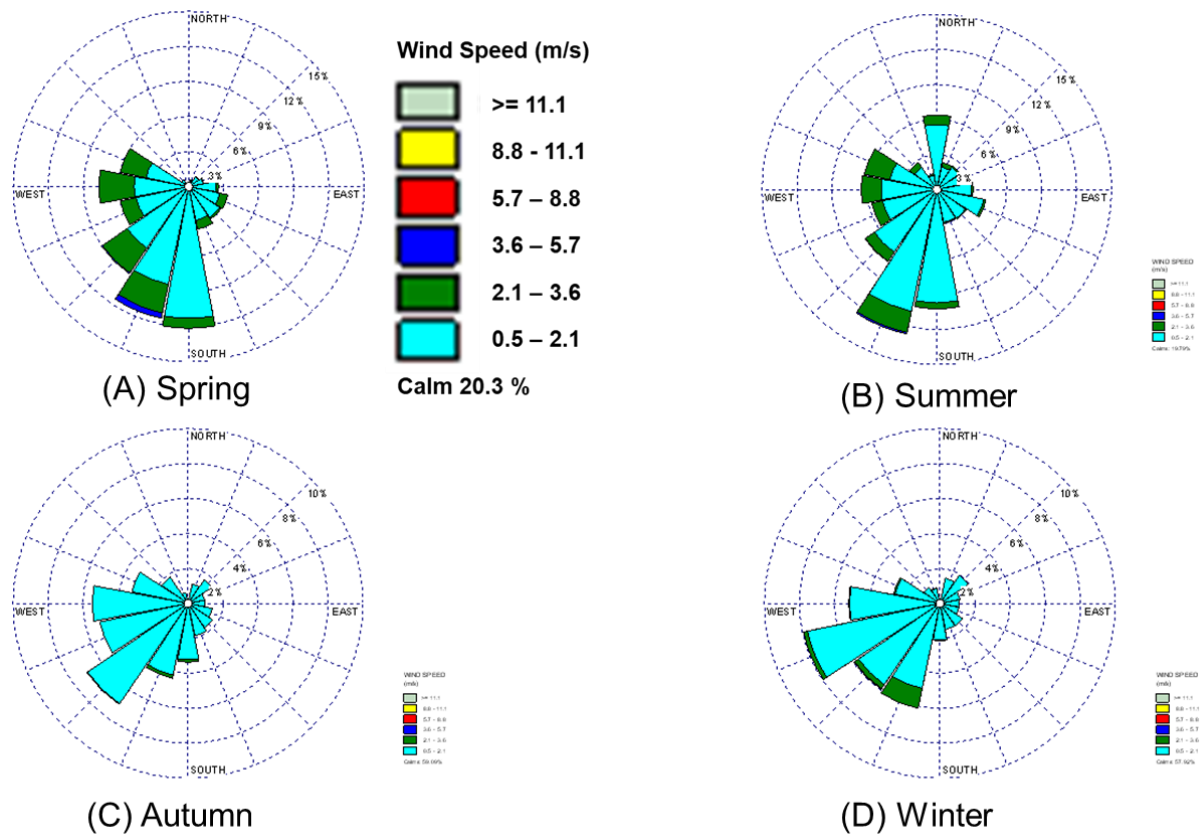


Figure 7: Windrose for the seasonal variation of wind speed and direction.

There are four distinct seasons in Kathmandu valley where the daily mean temperature varies from 10°C to 24°C . The highest temperature was recorded in the end of May to mid-June, and the lowest temperature was recorded in the month of January. Generally, the temperature of the valley varies from 2°C to 29°C , where winter is moderately cold and the rest of the seasons are cool. Approximately 1500 mm of rainfall has been recorded in the valley, where around 70% rain falls in the three months of the summer season, although there is a slight variation in each year. Moderately strong wind speeds (approximately 6 m/s) occur during the spring and summer seasons. Mostly, calm and moderately calm winds (wind speed of 0.5 m/s to 2.1 m/s) are evidenced during the autumn and winter, as shown in Figure 7. The lower temperature in the valley caused the formation of temperature inversion at the surface level, where the calm wind speed catalyzed the temperature inversion and caused accumulation of pollutants in a confined region.

4.2 Air quality of the Kathmandu Valley

Particulate matters such as PM10 and PM2.5, which have been monitored at Ratnapark, US-Embassy (Phora Durbar), Pulchowk, Bhaisipati, US-Embassy (Kathmandu), Shankhapark and Birendra School (Bhaktapur) were collected and analyzed to identify the monthly and seasonal variation of PM in the Kathmandu Valley, as in Figure 8. Due to the technical errors, there was PM10 data missing in the spring season, although the PM2.5 was recorded continuously. The data shows that the air pollution level was more than two times higher in the winter season (December, January, and February) than the spring season (March, April, and May) and the autumn season (September, October, and November). Moreover, the concentration of particulate matter was very low (both PM10 and PM2.5 were less than $20 \mu\text{g}/\text{m}^3$) as in Figure 8. There was more than 70% rainfall in the summer season only. The frequent rain may wash out the dust from the atmosphere as well as wash out the re-suspended dust from the surface.

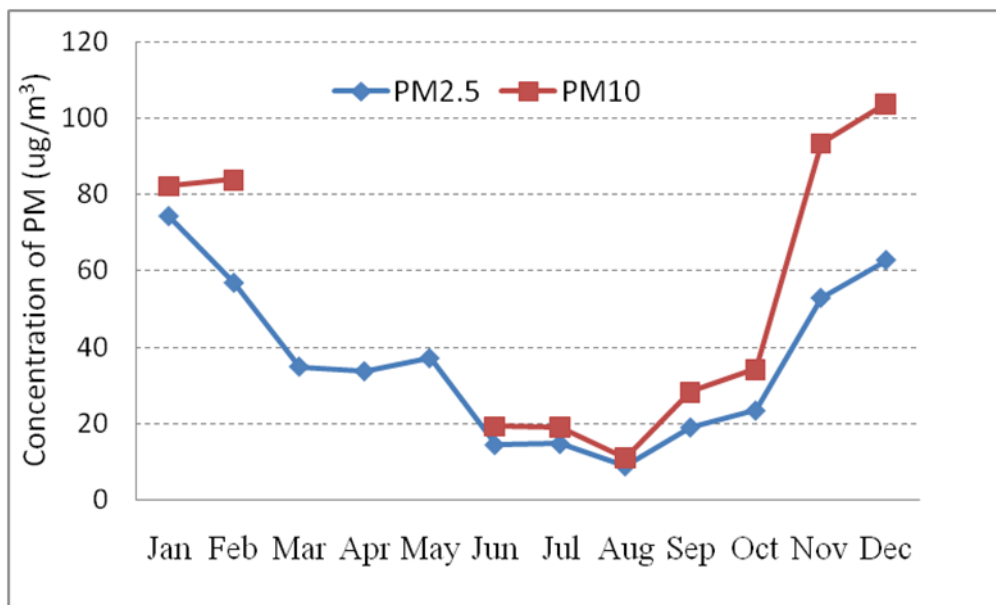


Figure 8: Monthly variation of the particulate matter in the Kathmandu Valley for the year 2018-2020.

4.3 Air flow/dispersion modeling

4.3.1.A Case study of the spring season

Mesoscale air flow/air dispersion modeling was carried out for the study area. Local air flow is generally produced due to the differential heating and cooling effect on the Earth's surface. In the Mountain / Valley area, a thermal circulation often develops due to the diurnal heating

and cooling of the mountain slopes. Solar radiation warms the Mountain slopes or Valley walls, which in turn warms the air in contact with it; the heated air (being less dense than the air at the same elevation above the Valley floor) rises as an upslope wind and is called the valley wind. Due to the outgoing radiation during the night, the mountain slopes cool more quickly than the Valley floor. The air in contact with the slopes and up to a certain depth generally cools through conduction and turbulent mixing. This cooler air flows down the slope and is called a slope or a mountain wind (Arya, 1999). The Valley wind is particularly strong in the south-facing slopes; however, the Valley is surrounded by high mountains, with most of the Mountain slopes facing the midday Sun, therefore, a significant amount of Mountain and Valley winds are developed. The surface elevation in the domain varied widely; it ranged from 78 m to 6688 m (maximum surface elevation above sea level). The internal modeling domain covered the Kathmandu Valley with a base elevation of approximately 1350 m from sea level; whereas, the surrounding mountains were approximately 2825 m (Nagarjun) from sea level.

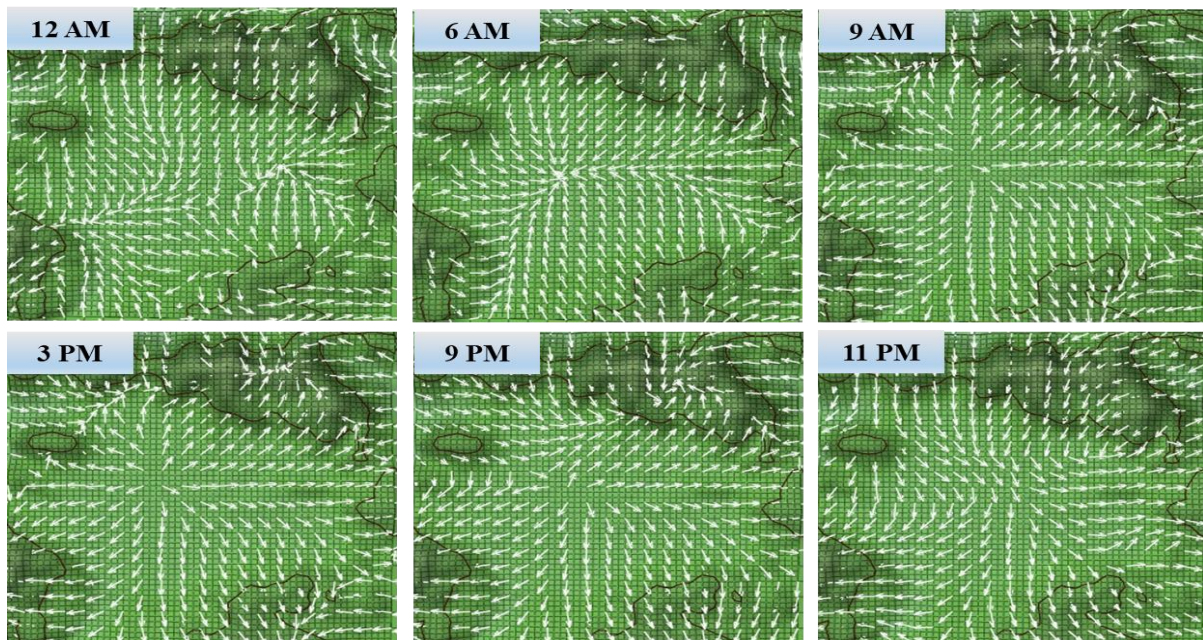


Figure 9: Wind flow vectors 10 m above the surface in the study domain at 12 AM, 6 AM, 9 AM, 3 PM, 9 PM and 11 PM.

Figure 9 shows the diurnal variation of the air flow vectors at different time intervals. Most of the Valley area was covered by the urban structure, and the mountain area was covered with the forest. After sunset, the mountain slopes released heat faster than the Valley surface, wherein the urbanization pattern and land-use type/material affect it and consequently influence on the airflow. Figure 9; 12 AM, 6 AM, and 11 PM show the breeze flow towards

the Valley (Mountain breeze), while Figure 12; 9 AM, 3 PM, and 9 PM show the breeze flow towards the mountain slopes (Valley breeze). The momentum of the breeze and its direction varied with time and geographical location. It is known that the intensity of solar radiation as well as the surface emissivity is time-dependent; however, surface elevation, land-use parameters, meteorological parameters, etc., vary with location.

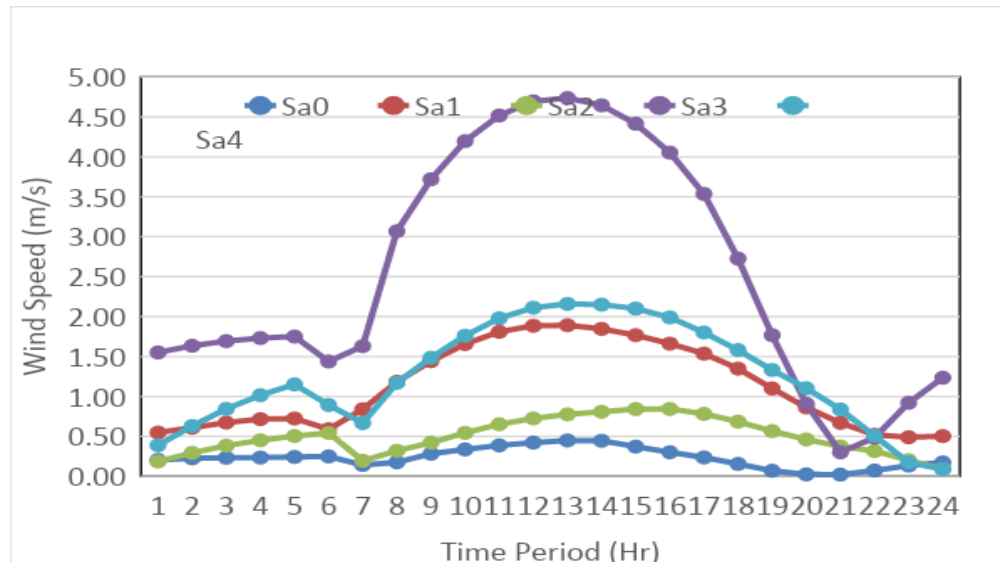


Figure 10: Diurnal variation of Mountain/Valley breeze at different sampling points; here the symbols represent as Sa0 (Ratnapark), Sa1 (Tahachal near to Ringroad), Sa2 (Bhaktapur), Sa3 (Near to Narayan Gopal Chowk) and Sa4 (Sunakothe, Lalitpur).

Figure 10 shows the diurnal variation of breeze flow for the monitoring points Sa0, Sa1, Sa2, Sa3, and Sa4. The momentum of the Valley breeze (up to 4.5 m/s) was more than double that of the mountain breeze (up to 1.8 m/s). Although the breeze momentum varies at different locations. With the decline of solar radiation in the evening, the breeze momentum reduced; it reached a calm condition around 9 PM. This could be referred to as a transition period. As the air pressure at the Valley surface became lower than the Mountain slopes, at around 11 PM, the Mountain breeze was generated; this Mountain breeze continued till 7 AM during the simulation period. The Mountain breeze gained maximum momentum just before sunrise, and it reached a transition stage between 7 and 8 AM. Due to the higher solar intensity, mountain slopes generally heat faster, and this in turn generates a significantly strong Valley breeze. Valley breeze gained maximum momentum at around 1 ~ 2 PM. The process repeats until the external air force or adverse climatic change does not occur.

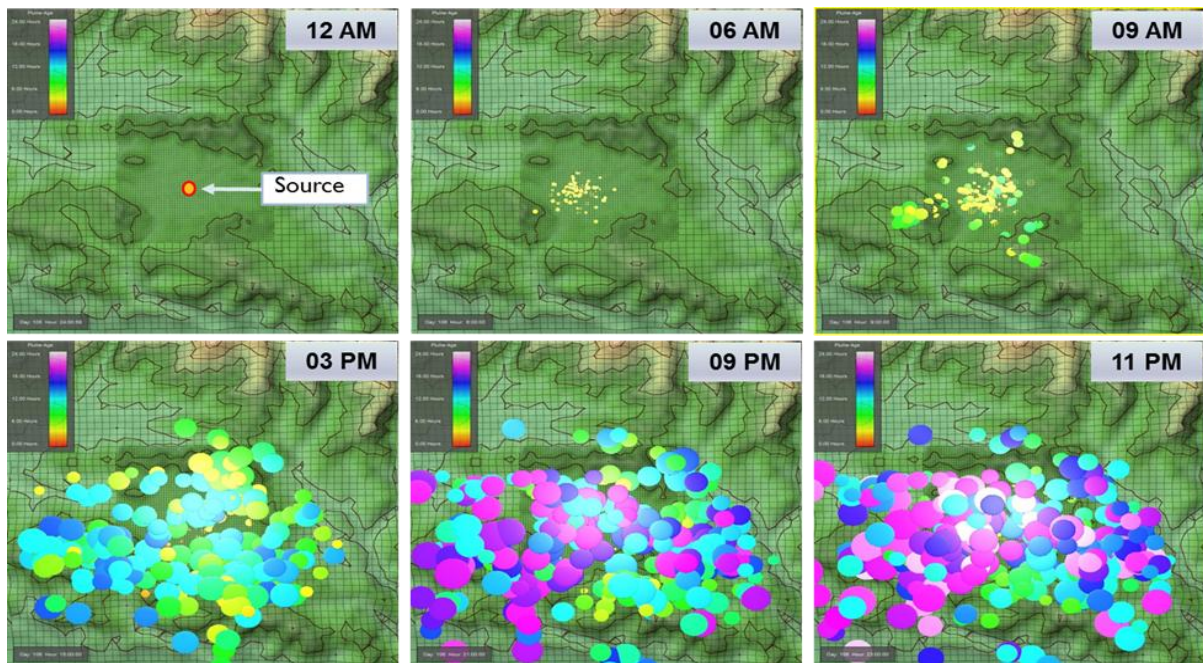


Figure 11: Puff dispersion mechanism from the point source in the Valley, wherein the puff source is at the central part of the Valley.

Puffs were emitted continuously from the point sources located at the central, eastern, southern, and northern parts of the Valley with a constant emission rate. Transport and dispersion mechanisms of the puffs from the point sources at different locations varied with the local air flow mechanism. The puffs emitted from the center of the Valley (southern part of KMC) disperse throughout the Valley; however, from midnight to early morning, the major portion of the puffs skewed towards the south-west direction, following the local air flow pattern as in Figure 11. The puffs emitted from the eastern part of the Valley were transported and dispersed in the eastern and south-eastern part of the Valley and its nearby mountain area (as in Figure 12). Similarly, the puffs emitted from the southern part of the Valley dispersed in the southern and south-eastern part of the Valley and its vicinity (as in Figure 13). Moreover, the puffs generated in the northern part of Metropolitan City were transported towards the valley area in the late night to the early morning, and it transported towards the uphill side in the daytime (as in Figure 14). The pollution transport and dispersion pattern in the Valley was affected by the local air flow characteristics. The smog generated in the eastern part of the mountainous area (touristic region) could be affected by the pollution transported from the central part and the eastern part of the Kathmandu Valley.

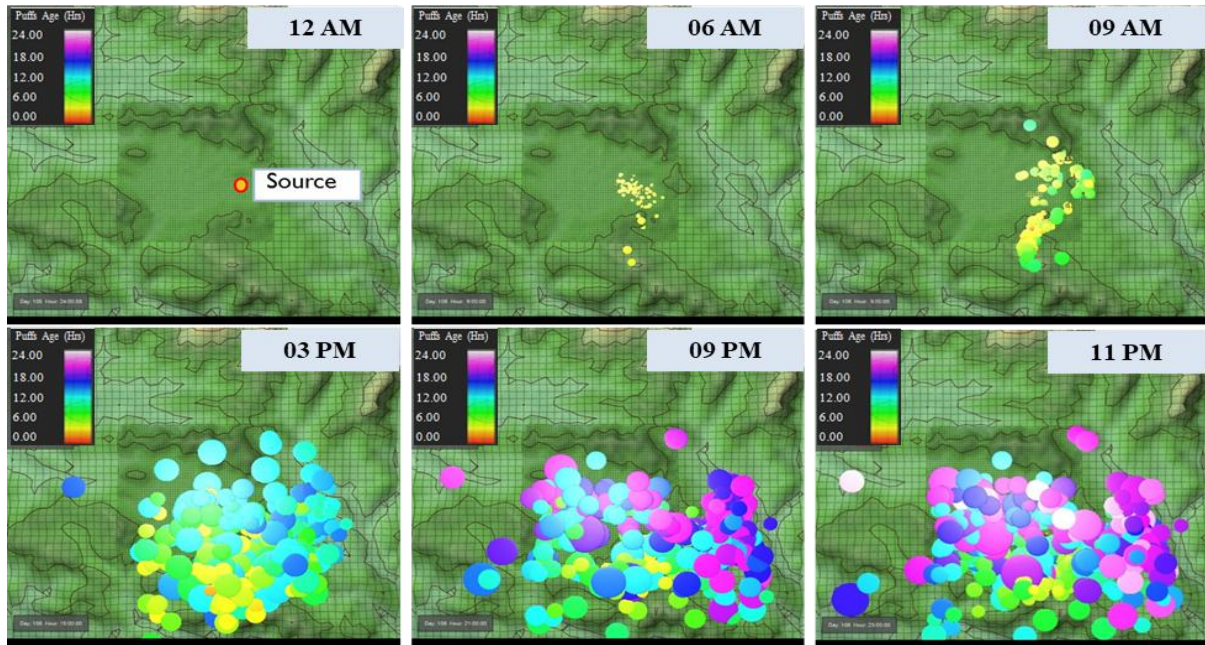


Figure 12: Puff dispersion mechanism from the point source, wherein the puff source is at the eastern part of the Valley.

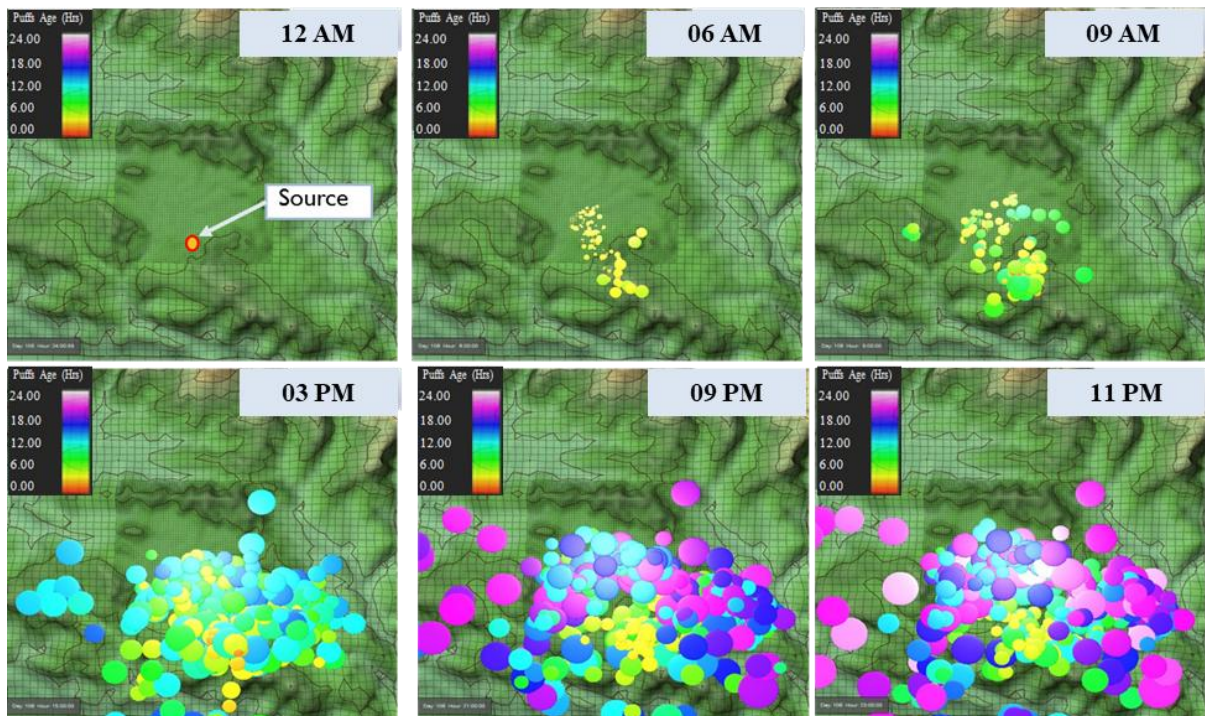


Figure 13: Puff dispersion mechanism from the point source, wherein the puff source is at the southern part of the Valley.

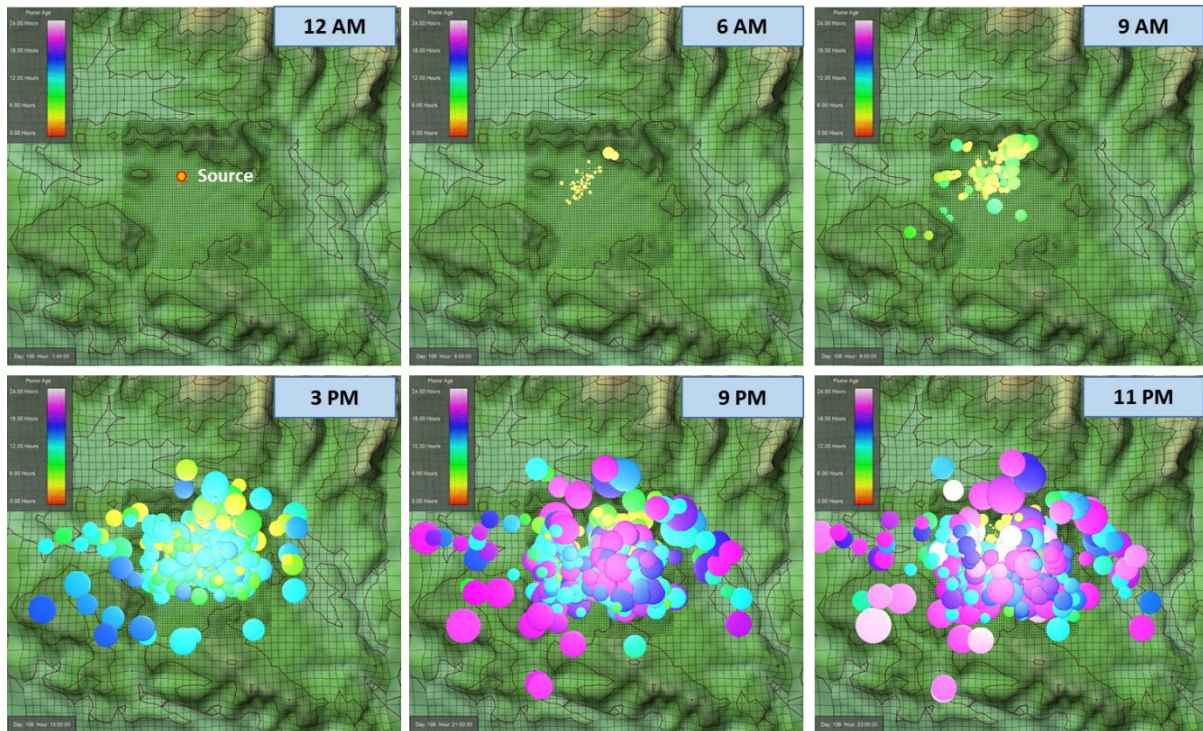


Figure 14: Puff dispersion mechanism from the point source in the Valley wherein the puff source is at the northern part of the Valley.

In the figure, the red color represents the younger puff and the white color represents the aged puff. As the puffs become older, the puff's size gradually expands and color also transforms towards white, as in Figures 11 – 14. The majority of the puffs in the surface area of the Valley mostly follow the breeze path. The aged puff dispersed at higher altitudes and wider areas where the breeze impact was least. Moreover, a large number of puffs capped the Valley top. This was because, as shown in Figure 11, the puff source was at the central part of the Valley, where most of the puffs were dispersed in the Valley area. This shows that understanding the air flow characteristics and air flow corridor could be helpful for managing the air quality of the Kathmandu Valley. This study also suggests that the north-to-south air flow is common in the study area; moreover, the air flow corridors are at the southern, south-eastern part of the Valley.

4.3.2 Impact of landuse change on breeze flow

Even if the solar incoming radiation is constant in nearby areas, the temperature of the Earth's surface differs significantly from place to place due to the different landuses and characteristics i.e., anthropogenic heat, specific heat capacity, albedo, etc., of the objects covering the land surface. After the sunset, the mountainous surface releases heat faster than the valley basin;

therefore, the temperature of the mountain slope becomes lower than the valley basin from late evening to the early morning. After the sunrise, the air flow phenomenon becomes reversed. When the irrigated crop land changes to the urban land, the surface characteristics such as soil moisture, specific heat capacities, albedo, anthropogenic heat emission, etc., also change. It consequently affects local wind characteristics. Figure 15 shows the breeze flow at different sampling locations when the valley land surface is covered with irrigated crop land, and Figure 16 shows the breeze flow pattern when the valley land surface changes to urban land. The results show that the local breeze becomes stronger during the day and weaker during the night when the irrigated crop land changes to the urban land.

In other words, there is a chance of the development of an urban heat island in the downtown area that increases the temperature of the urban area, which can be distinctly observed at nighttime. Major and densely urbanized cities such as Tokyo, Seoul, Taipei, etc. have already experienced the heat island effects. The daily average wind speeds at different sampling points do not vary significantly with the change of landuse pattern as in Figure 17.

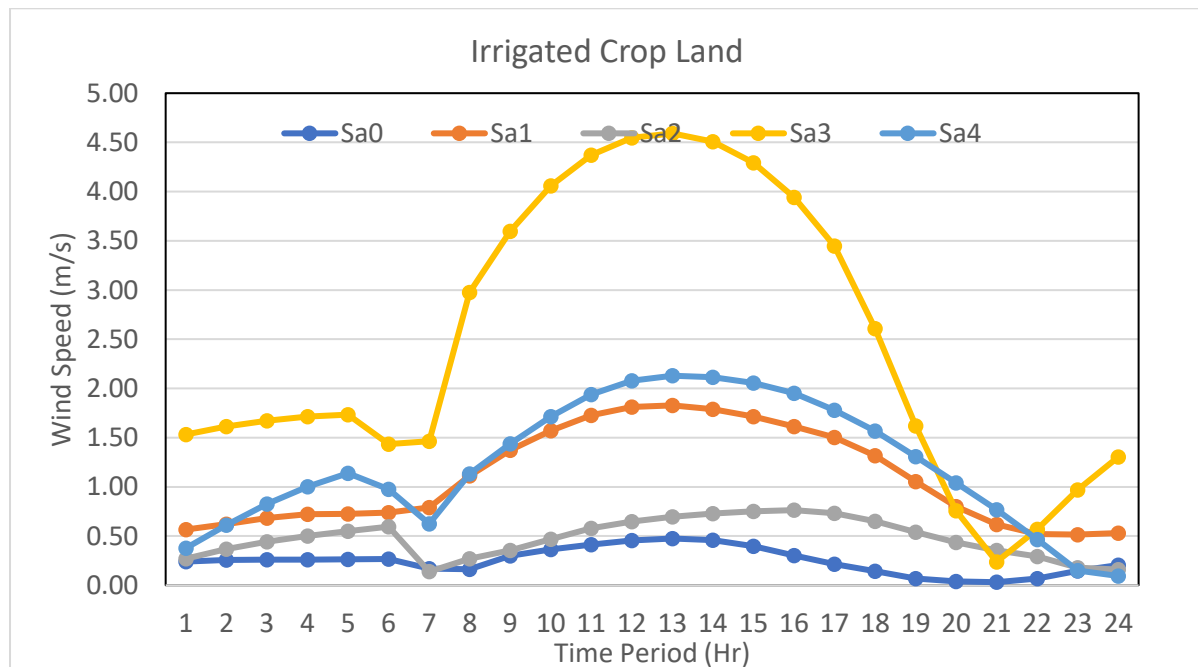


Figure 15: Diurnal variation of wind speed (Irrigated crop land).

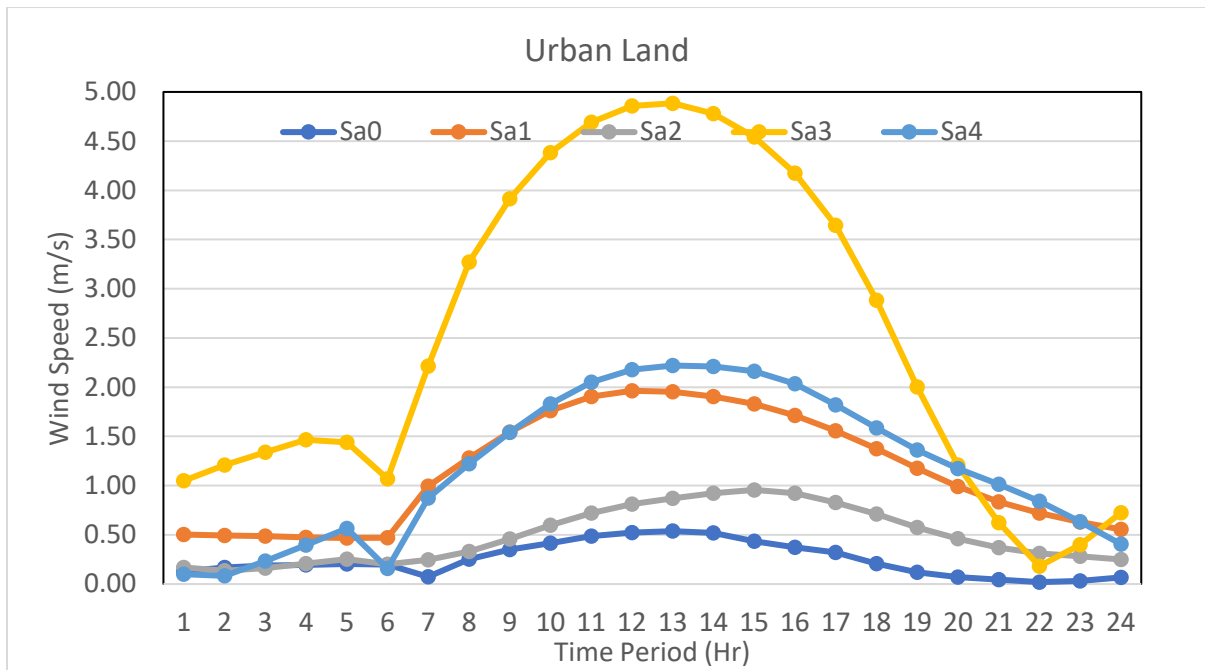


Figure 16: Diurnal variation of wind speed (Urban landuse).

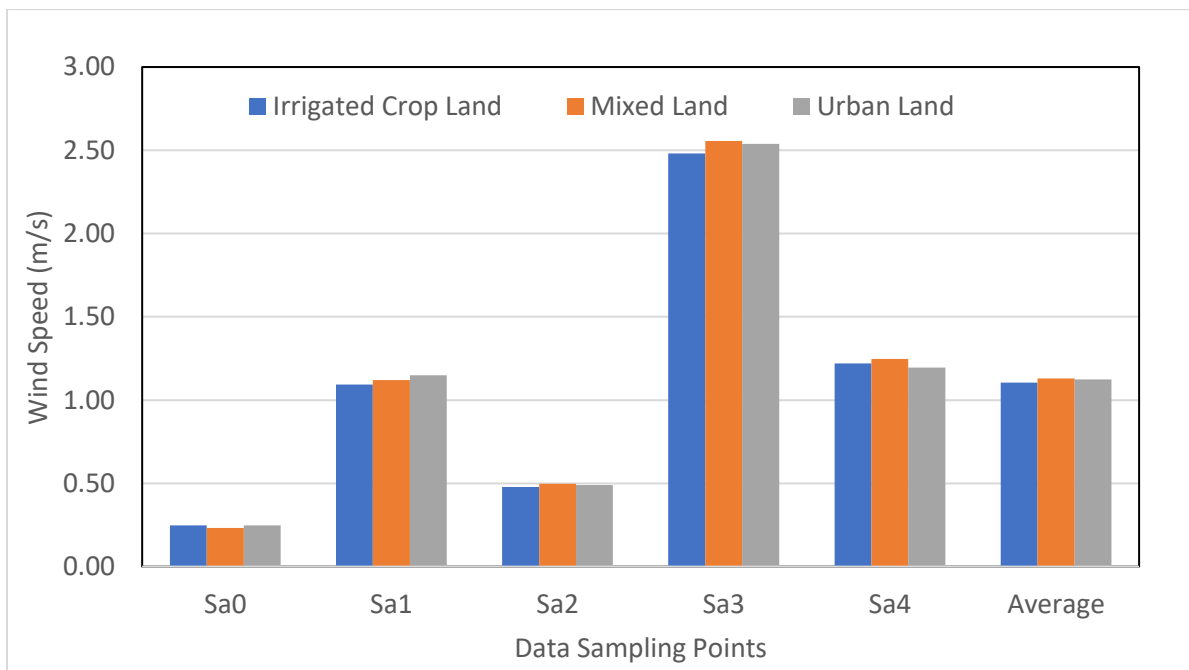


Figure 17: Comparison of average wind speed for different cases at various sampling locations.

5. Conclusion and Recommendation

Air quality management in the Kathmandu Valley remains an exceptionally complex and pressing challenge, shaped by the interplay of diverse emission sources, valley-specific topography, meteorological conditions, and transboundary influences. This study demonstrates

that soil-based dust and combustion-derived pollutants are the dominant contributors to ambient air pollution, largely originating from construction and demolition activities, agricultural practices, and vehicular movement on unpaved or poorly maintained roads. The dispersion modeling results reveal that calm wind conditions prevailing in the central valley inhibit pollutant transport, leading to prolonged accumulation of emissions near their sources and a sustained deterioration of air quality. In contrast, emissions generated in the southern and southeastern sectors exert comparatively limited influence on the overall pollution burden, suggesting spatial variability in pollution impacts. These findings underscore the necessity of coordinated and integrated air quality management across Kathmandu Metropolitan City (KMC) and its neighboring municipalities, as isolated interventions are unlikely to yield meaningful or lasting improvements.

The study further highlights the critical importance of spatial planning, source decentralization, and technology transition in mitigating air pollution in the Valley. Strategic relocation of pollution-intensive development projects toward climatically favorable zones, decentralization of emission sources away from the core urban area, and a rapid shift from fossil-fuel-based public transport to electric mobility emerge as key long-term solutions. Complementary measures—including urban greening, preservation of agricultural land, promotion of pervious surfaces, and incorporation of air pollution hazards into multi-hazard risk-sensitive land-use planning—are essential for addressing both air quality degradation and associated urban heat island effects. Moreover, strict regulation of construction and demolition activities, improved road design and maintenance, reliable vehicle emission testing with enforceable penalties, and public awareness programs targeting open waste burning and forest fires are indispensable policy priorities. Collectively, these integrated and evidence-based interventions provide a robust framework for policymakers to advance sustainable urban development while progressively improving air quality in the Kathmandu Valley.

Acknowledgements

This work was partially supported by the Mayor's Research Fellowship 2020, Kathmandu Metropolitan City. The author would like to acknowledge Prof. Dr. Ram Kumar Sharma and all the CPC members. The author would like to acknowledge the Asian Institute for Environmental Research and Energy for providing the simulation software. Paraphrasing and language correction were done using OpenAI.

References

- Chang, C.C., Tsai, S.S., Ho, S.C., Yang, C.Y. (2005) Air pollution and hospital admissions for cardiovascular diseases in Taipei. Taiwan, Environmental Research 98, 114-119.
- Copper, C.D., Alley, F.C. (2002) Air Pollution Control: A design approach. Waveland Press Inc., USA.
- Donaldson, K., MacNee, W. (2001) Potential mechanism of adverse pulmonary and cardiovascular effects of particulate air pollution (PM10). International Journal of Hygienic and Environmental Health 203, 411-415.
- ENPHO (2001) Status of brick kiln in Kathmandu valley. Environment and public health organization (ENPHO), Kathmandu.
- Goldberg, M.S., Burnett, R.T., Yale, J.F., Valois, M.F., Brook, J.R. (2006) Association between ambient air pollution and daily mortality among persons with diabetes and cardiovascular disease. Environmental Research 100, 255-267.
- Kan, H., Chen, C. (2003) Air pollution and daily mortality in Shanghai: a time-series study. Archives of Environmental Health 58, 360-367.
- KVAQMP (2076) Kathmandu Valley Air Quality Management Action Plan 2076.
- Panday, A.K., Prinn, R.G. (2009a), Diurnal cycle of air pollution in the Kathmandu Valley, Nepal: Observations. Journal of Geophysical Research 114, D09305.
- Panday, A.K., Prinn, R.G., Schar, C. (2009b) Diurnal cycle of air pollution in the Kathmandu Valley, Nepal: 2. Modeling results. Journal of Geophysical Research 114, D21308, doi:10.1029/2008JD009808.
- Pandey, A. (2006) The diurnal cycle of air pollution in the Kathmandu Valley, Nepal. Ph.D. thesis, Massachusetts Institute of Technology, US.
- Pokhrel, R. & Lee, H. (2014) Integrated Environment Impact Assessment of Brick Kiln using Environmental Performance Scores. Asian J. Atmos. Environ 8, 15–24. <https://doi.org/10.5572/ajae.2014.8.1.015>
- Pokhrel, R. (2025) Study of air pollution and its dispersion pattern in Pokhara Valley. Pokhara Engineering College Journal 2 (1), 11 – 22. DOI: [10.3126/pecj.v2i1.76827](https://doi.org/10.3126/pecj.v2i1.76827)
- Pokhrel, R., Lee, H. (2011) Algorithm development of visibility monitoring using digital image analysis. Asian Journal of Atmospheric Environment 5-1, 8-20. DOI: [10.5572/ajae.2011.5.1.008](https://doi.org/10.5572/ajae.2011.5.1.008)

- Pokhrel, R., Lee, H., Sharma, R.K. et al. (2021) Aerosol Dispersion Over a High Altitude Region: a Case Study of Kathmandu, Nepal. *Water Air Soil Pollut* 232, 80. <https://doi.org/10.1007/s11270-021-05007-4>
- Pudasainee, D., Sapkota, B., Bhatnagar, A., Kim, S.H., Seo, Y.C. (2010) Influence of weekdays, weekends and bandhas on surface ozone in Kathmandu valley. *Atmospheric Research*, 95, pp. 150-156.
- Regmi, R.P., Kitada, T., Kurata G. (2003) Numerical simulation of late wintertime local flows in Kathmandu Valley, Nepal: implication for air pollution transport. *Journal of Applied Meteorology* 42, 389-403.
- Sapkota, B., Dhaubadel, R. (2002) Atmospheric turbidity over Kathmandu Valley. *Atmospheric Environment* 36, 1249-1257.
- Sharma, C.K. (1997) Urban air quality of Kathmandu Valley “Kingdom of Nepal”. *Atmospheric Environment* 31, 2877-2883.
- Shrestha, R.M., Malla, S. (1996) Air pollution from energy use in developing country city - the case study of Kathmandu valley, Nepal. *Clean Air Initiative* (http://cleanairinitiative.org/portal/system/files/articles-58928_resource_1.pdf).
- World Bank (1997) *URBAIR - Urban air quality management strategy in Asia: Kathmandu valley report*, New York, USA